Tectonophysics, 165 (1989) 251–268
Elsevier Science Publishers B.V., Amsterdam – Printed in The Netherlands

Geodynamics of an arc–ridge junction: the case of the New Hebrides Arc / North Fiji Basin

P. MAILLET [1], M. MONZIER [2], J.-PH. EISSEN [1] and R. LOUAT [2]*

[1] *ORSTOM B.P. 70, 29263 Plouzané (France)*
[2] *ORSTOM B.P. A5, Nouméa Cédex (New Caledonia)*

(Received July 14, 1988; revised version accepted October 20, 1988)

Abstract

Maillet, P., Monzier, M., Eissen, J.-Ph. and Louat, R., 1989. Geodynamics of an arc–ridge junction: the case of the New Hebrides Arc/North Fiji Basin. *Tectonophysics*, 165: 251–268.

Detailed surveys (bathymetry, magnetism, seismicity and focal mechanism solutions) recorded on the junction between the southern New Hebrides Arc and the North Fiji Basin enlighten the geodynamic complexity of the area.

The presently active c. N–S-oriented spreading structures of the North Fiji Basin are superimposed on ancient ones, which appeared during a N135°E spreading episode active before 3 Ma. A recent southward extension of the New Hebrides Arc occurred c. 2 Ma ago.

Structural and geophysical consequences of both events partly obscure the present arc–ridge junction. For example, back-arc troughs do not exist to the south of the former arc termination. N45°E structural directions, present all over the studied area, are interpreted as older transform faults related to the N135°E spreading axis, which also left recognizable NW–SE magnetic anomalies.

However, the New Hebrides Arc/North Fiji Basin junction remains geodynamically unstable, due to the concomitance of convergent, strike-slip and divergent movements. Their respective crustal expressions, i.e. arc volcanism, lateral displacements and seafloor spreading, are examined and considered in their regional environment.

A provisional model of the arc-ridge junction that accounts for most of the parameters analysed above is presented.

Introduction

The New Hebrides Arc/North Fiji Basin arc–ridge junction is discussed in this paper, using new maps presenting the bathymetry, magnetism, seismicity and focal mechanisms of this area. As a background, some relevant features of the New Hebrides Arc (NHA) and of the North Fiji Basin (NFB) are summarized below.

The New Hebrides Arc

The New Hebrides trench marks the subduction of the India–Australia Plate under the NFB (Fig. 1), with a convergence rate of 10 cm/yr and a subduction strike of N70°E (Dubois et al., 1977). Seismological studies indicate a generally steep (c. 60°), northeastward-dipping, continuous subducting slab along the NHA (Coudert et al., 1981; Isacks et al., 1981; Louat et al., 1982). South of 20°S, the maximum length of the Benioff zone abruptly shortens from 300 to 200 km (Louat et al., 1988), its dip decreases, and two hinge zones may tear the downgoing plate between 22° and 23°S (Monzier et al., 1984b).

* All in GIS (Groupement d'Intérêt Scientifique) "Océanologie et Géodynamique", GS 410012.

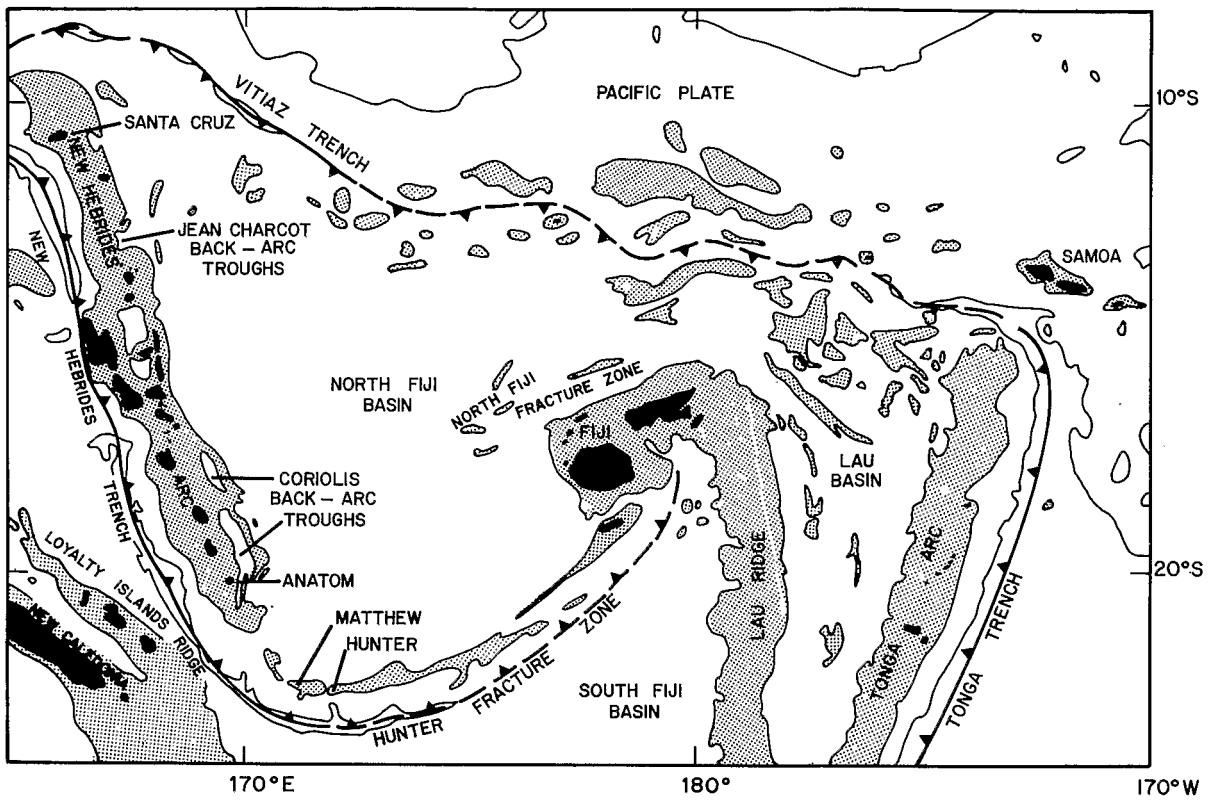

Fig. 1. Bathymetric sketchmap of the South West Pacific, after Brocher and Holmes (1985). Stippled areas correspond to 0–2 km depths.

The NHA comprises three volcanic chains: a western belt (upper Oligocene to middle Miocene); an eastern belt (Mio-Pliocene); and a central chain running over c. 1500 km from Santa Cruz islands to Matthew and Hunter volcanoes. This Quaternary and still active volcanic chain is mainly made up of basalts and basaltic andesites (Carney et al., 1985). By contrast, the two southernmost active volcanoes, Matthew and Hunter, are made up of calc-alkaline orogenic andesites (Maillet et al., 1986a).

Recent studies of the New Hebrides back-arc troughs (Jean-Charcot troughs in the north, Coriolis troughs in the south) have defined their location and structure (Récy et al., 1986), their volcanic history (Monjaret et al., 1987) and their relationships with the evolution of the NHA and the NFB (Charvis et al., in prep.). These back-arc troughs are absent south of Anatom island (Fig. 1). Roughly at the same latitude, the central volcanic chain, bounded by the 2-km isobath, almost disappears between 21°S and Matthew island (Monzier et al., 1984a); and the width of the shallow interplate seismicity zone rapidly narrows south of Anatom island (Louat et al., 1988).

The North Fiji Basin

Located between the NHA and the Fiji platform, the NFB is limited to the north by the Vitiaz trench, and to the south by the Hunter fracture zone (Fig. 1). Recent studies give new insights on the tectonic configuration of this active marginal basin, the main characteristics of which have been summarized by Auzende et al. (1988a, b) for its central and southern parts, and by Brocher and Holmes (1985) for its northern part.

In the southern part of the NFB, underway magnetic surveys confirm the presence of an active N–S spreading center between 20°S and 20°30′S, at 173°25′E, with a full spreading rate of 6 cm/yr between anomalies 2 and J, and 8 cm/yr between anomalies J and 1 (Maillet et al., 1986b; and see Fig. 2). Magnetic anomalies older

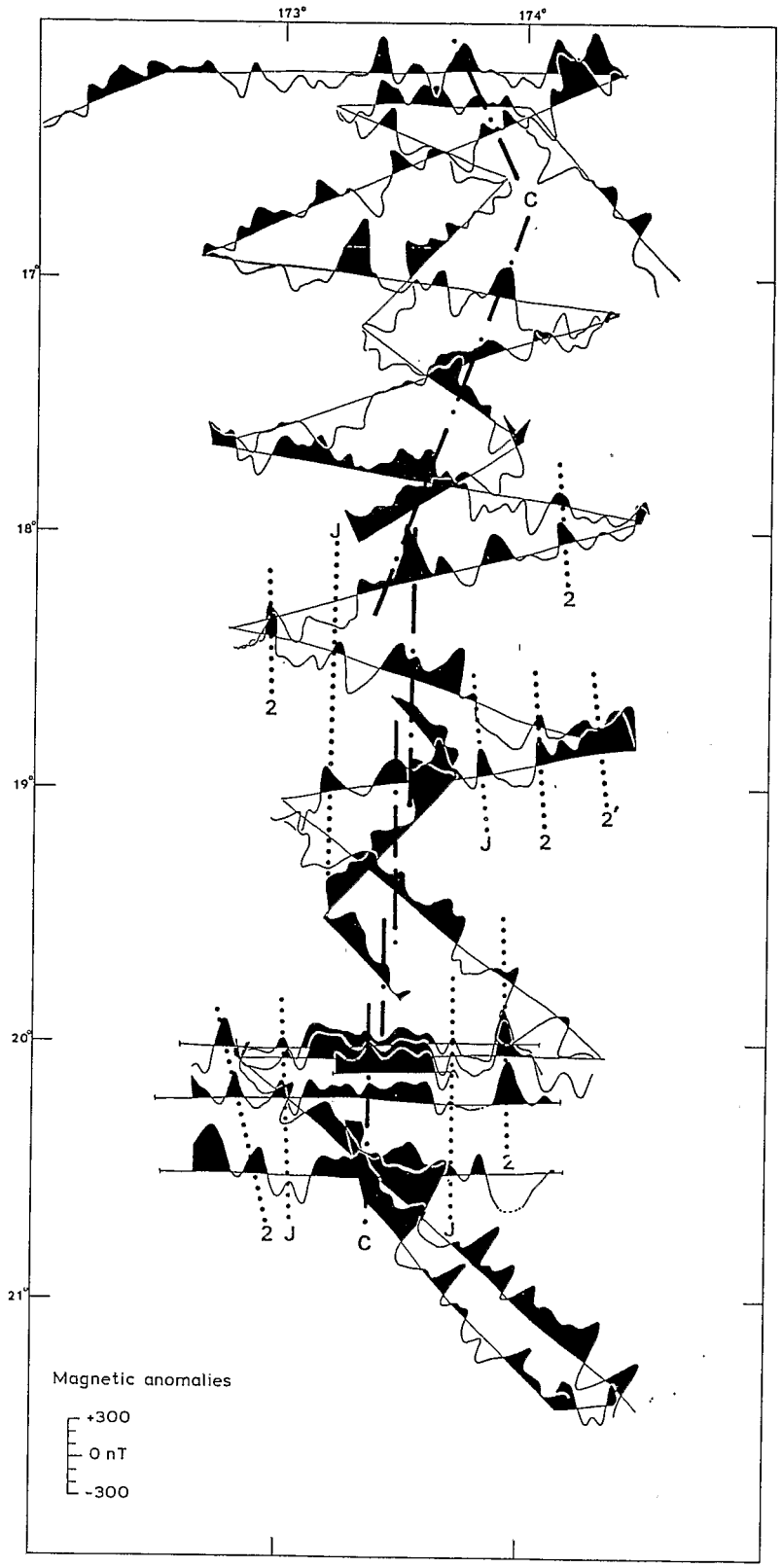

Fig. 2. Magnetic profiles across the North Fiji Basin spreading axis and interpreted magnetic lineations. *C* stands for anomaly 1 (i.e. central anomaly). From Auzende et al. (1988a).

than anomaly 2 show NW–SE orientations, indicating a major change in the NFB spreading system at c. 2 Ma. South of 21°S, anomaly J is less distinct, but anomaly 1 (corresponding to the spreading axis) can be identified on a c. N–S-oriented ridge, located near 174°E between 21°S and 21°30′S, i.e. c. 80 km to the east of the above N–S axial spreading center. The 173°25′E spreading ridge is probably propagating to the south, at the expense of the segment located near 174°E (Maillet et al., 1986b).

North of 20°S, three main structural areas can be defined:

(a) Between 20°S and 18°30′S, the NFB spreading center can be tracked along a roughly N–S direction at c. 173°25′E. Overlapping spreading centers have been recognized along this portion of the ridge. This axial domain is cut by N45°E transverse structures every c. 40 km, which sometimes offset the axis by several kilometers (Auzende et al., 1988a, b). These N45°E structural directions correspond to shallow crustal remnants of movement linked to the 30° clockwise rotation of the NHA during the past 6 Ma (Falvey, 1978; Malahoff et al., 1982a, b), i.e. they represent ancient transform faults linked to the former N135°E spreading system, active during the rotation. Magnetic anomaly profiles confirm the presence of a central, c. N–S-oriented, anomaly, the width of which varies from 50 to 60 km. In this area, the track of anomalies 1, J and 2 give a full spreading rate varying from 6.8 cm/yr in the north to 8.2 cm/yr in the south (Fig. 2; Auzende et al., 1986a, 1988a, b). These figures are in good agreement with those proposed for the area south of 20°S (Maillet et al., 1986b). Although located by Auzende et al. (1988a, b), the presence of an anomaly 2′ on the eastern limb of the NFB spreading system at 19°S (Fig. 2) remains questionable as far as the present authors are concerned. However, correlation of anomalies older than anomaly 2′ in the central NFB show c. NW–SE directions (Auzende et al., 1988c). As noted before, this also has been observed in the southern NFB south of 20°S for anomalies older than anomaly 2 (Maillet et al., 1986b). Therefore, the age of the anomalies 2–2′, i.e. 2–3 Ma, probably corresponds to an abrupt change in the NFB spreading system, from N135°E before 3 Ma, to roughly N–S thereafter.

(b) Between 18°30′S and 17°S, the NFB spreading ridge trends N15°–20°E. The limit between these two areas may correspond to a propagating rift (Gente, 1987), the northern ridge (N15°E) being younger than the southern one (N–S), induced by a recent (< 1 Ma) local rearrangement (Lafoy et al., 1987).

(c) North of 17°S, a triple junction, centered at 174°E, 16°40′S, corresponds to the mutual interaction of the above N15°–20°E ridge with another N160° active ridge and with the westernmost extension of the North Fiji fracture zone (Auzende et al., 1986b, 1988a, b; Kroenke et al., 1987; Lafoy et al., 1987).

New data

Bathymetry

A new bathymetric map (Fig. 3c) is presented here which extends and partly completes a former one (Monzier et al., 1984a) limited at 173°E. Stippled areas on the track-lines figure (Fig. 3a) correspond to areas which have been surveyed using a multi-narrow-beam echosounder (Seabeam) during the 1985 cruises of R/V "Jean Charcot" (the PROLIGO cruise and legs 1–3 of the SEAPSO cruise: Daniel et al., 1986; Récy et al., 1986; Auzende et al., 1986a). All other surveys have been carried out mainly using the R/V "Coriolis" (or the R/V "Vauban" in the vicinity of Matthew and Hunter volcanoes), using a 12-kHz wide-beam echosounder and a "TRANSIT" satellite positioning system. The toponyms of the studied area appear on Fig. 3b.

The trench (more than 6 km deep) can be mapped up to 172°30′S, and marks the boundary between the NFB and the South Fiji Basin at 23°S. The volcanic chain changes in morphology south of 21°10′S, and almost disappears between the Gemini seamounts and the Matthew and Hunter ridge. N165°E-oriented subvertical faults, with a dextral component, displace the global E–W trend of the Matthew–Hunter ridge between 171°E and 172°30′E. This ridge is abruptly interrupted near 173°E, 22°10′S, and relayed, to the

east of 173°E, by a N70°E ridge, which marks the onset of the active Hunter fracture zone (Monzier et al., 1984b).

The bathymetric map of the southern part of the NFB reveals structural directions related to a spreading pattern (Fig. 3c). Isobaths in the area 172°40′–174°E/20–21°S emphasize the N–S spreading zone, centered along the 2800-m isobath at c. 173°25′E (Maillet et al., 1986b). The 3-km isobath in this area is fan-shaped, symmetrically widening to the north. This part of the spreading ridge is offset eastward by c. 80 km at 20°45′S through a c. N45°E fracture zone. South of this fracture zone, the axial spreading ridge can be tracked along a N–S direction near 174°E, down to 21°45′S, where it abruptly disappears.

Two groups of oblique structures also appear on Fig. 3c.

In the southeastern part of the map, between 174–176°E/21–22°S, prominent directions are N70°E. As noted by Monzier et al. (1984b), these directions correspond to the general direction of the Hunter fracture zone, which separates the c. 4–5 km deep South Fiji Basin from the shallower (2–3 km deep) NFB.

Ridges and troughs trending N40–50°E are also frequent. These oblique directions have been found further north along the N–S spreading axis of the central NFB (Auzende et al., 1988a, b). They also affect the inner slope of the New Hebrides trench around 170°E, 22°S. Moreover, the N45°E directions correspond to the direction of extension recognized in the northern New Hebrides back-arc troughs, the Jean-Charcot troughs (Charvis et al., in prep.), and are close to the direction of extension (N30°E; Récy et al., 1986) observed in the southern back-arc troughs, the Coriolis troughs. Thus, N45°E oblique structures observed in the southern NFB can be linked to the general N30–45°E extension regime proposed by Charvis et al. (in prep.) for the whole NFB. They represent fossil transform faults of a former spreading system, active in the central NFB before 3 Ma.

Magnetism

The general pattern of positive (black) and negative (white) magnetic anomalies deduced from profiles recorded at sea is shown in Fig. 4. These data have essentially been obtained during ORSTOM cruises (EVA programme) and recently during the ORSTOM–IFREMER SEAPSO cruises (legs 1–3, 1985) of R/V "Jean-Charcot". Correlation of positive and negative anomalies, respectively, between profiles, leads to a general map of magnetic anomalies in the southern NFB and New Hebrides Arc, which adjoins, to the south and to the west, the maps published by Cherkis (1980) and Malahoff et al. (1982a), using aeromagnetic data. The analysis of this map leads to several observations.

The southern New Hebrides trench is generally marked by a positive magnetic anomaly, which disappears around 172°25′E, 23°10′S. This area also corresponds to the deepest zone (7575 m) of the southern New Hebrides trench (Fig. 3), and may mark the southeastern limit of the convergent movement linked to the subduction.

The central positive anomaly of the NFB can be followed to 20°50′S along a c. N–S direction between 173°E and 174°E. It is fan-shaped, widening to the north, and can be correlated with the bathymetric contours of Fig. 3c.

The N45°E fracture zone, which offsets the southern NFB ridge between 173°E and 174°30′E near 20°45′S (Fig. 3c), is marked by a negative anomaly (Fig. 4).

The positive anomaly centered at 174°05′E between 20°50′S and 21°45′S (Fig. 4) is the southernmost magnetic expression of the NFB spreading ridge, which is thus offset to the east by c. 80 km. This central magnetic anomaly, about 43 km wide, probably represents anomaly 1 lasting 0.7 Ma. This gives a full spreading rate of c. 6 cm/yr. East of this central anomaly, a narrow, elongate positive anomaly is observed near 174°30′E between 20°25′S and 21°10′S. It is postulated that this anomaly represents anomaly 2 (c. 2 Ma) of the same spreading axis, which is then located at c. 40 km of the central anomaly. This would correspond to a half-spreading rate of c. 2 cm/yr during the past 2 Ma.

Although these figures are hypothetical, they support the idea of a regressive rift south of 20°50′S, compared to the northern limb.

The central anomaly is relayed to the south, at

22° S between 172° E and 174° 30′E, by a series of N70° E-trending positive and negative anomalies which are probably related to the Hunter fracture zone.

In addition to N–S anomalies related to the actual NFB spreading system, Fig. 4 shows c. N135° E anomalies (for example near 173° E, 21° S and 175° E, 20° 30′S) which correspond to N45° E

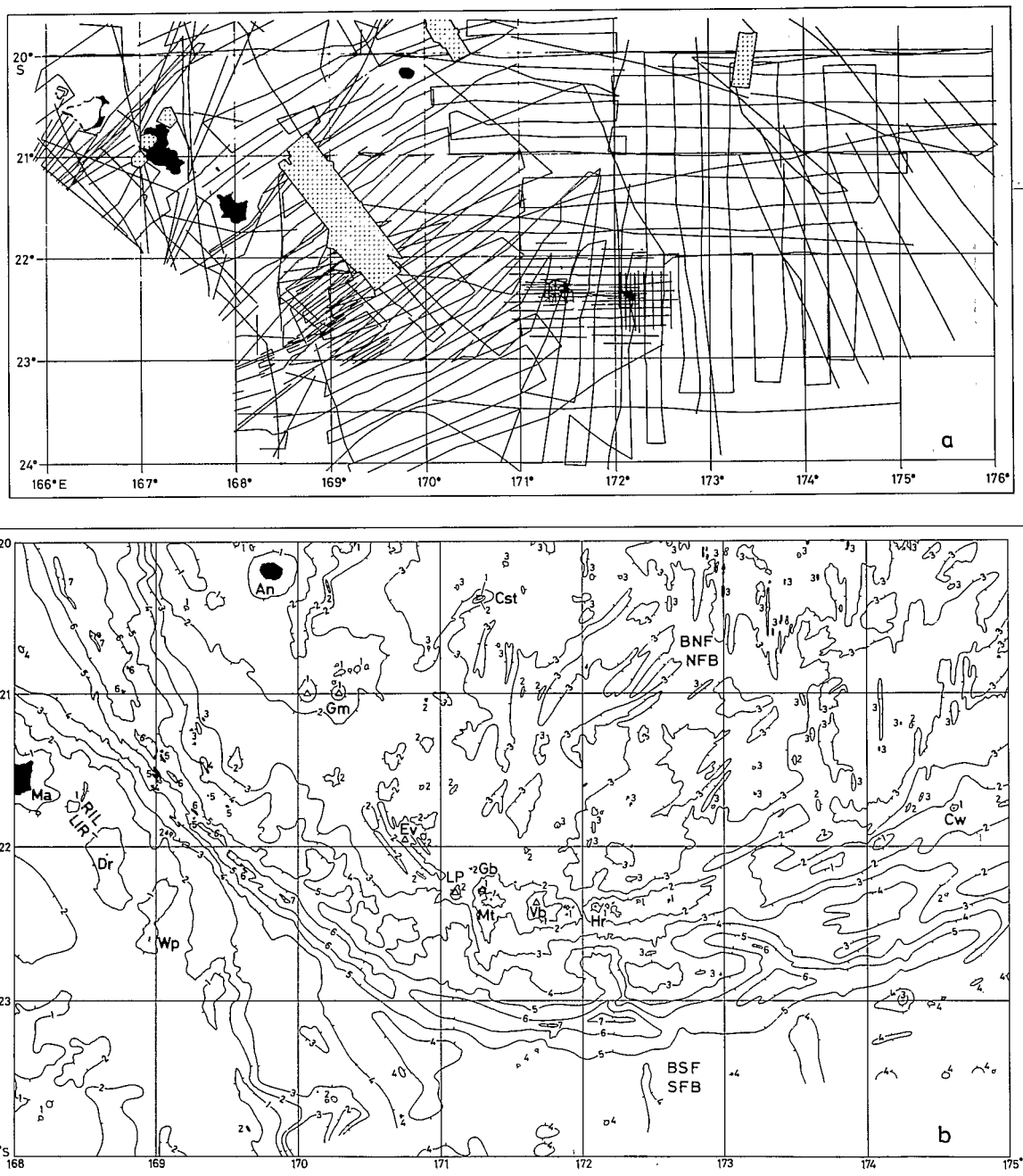

Fig. 3. Bathymetry of the southern New Hebrides island arc and southern North Fiji Basin. a. Tracklines figure. b. Toponyms of the studied area (bathymetry from Fig. 3c). *Ma*—Mare; *Dr*—Durand Reef; *Wp*—Walpole; *LIR/RIL*—Loyalty Islands Ridge; *SFB/BSF*—South Fiji Basin; *An*—Anatom; *Gm*—Gemini Seamounts; *Ev*—Eva Seamounts; *LP*—La Pérouse Seamount; *Gb*—Gilbert Seamount; *Mt*—Matthew Volcano; *Vb*—Vauban Seamount; *Hr*—Hunter Volcano; *Cw*—Conway; *Cst*—Constantine Bank; *NFB/BNF*—North Fiji Basin.

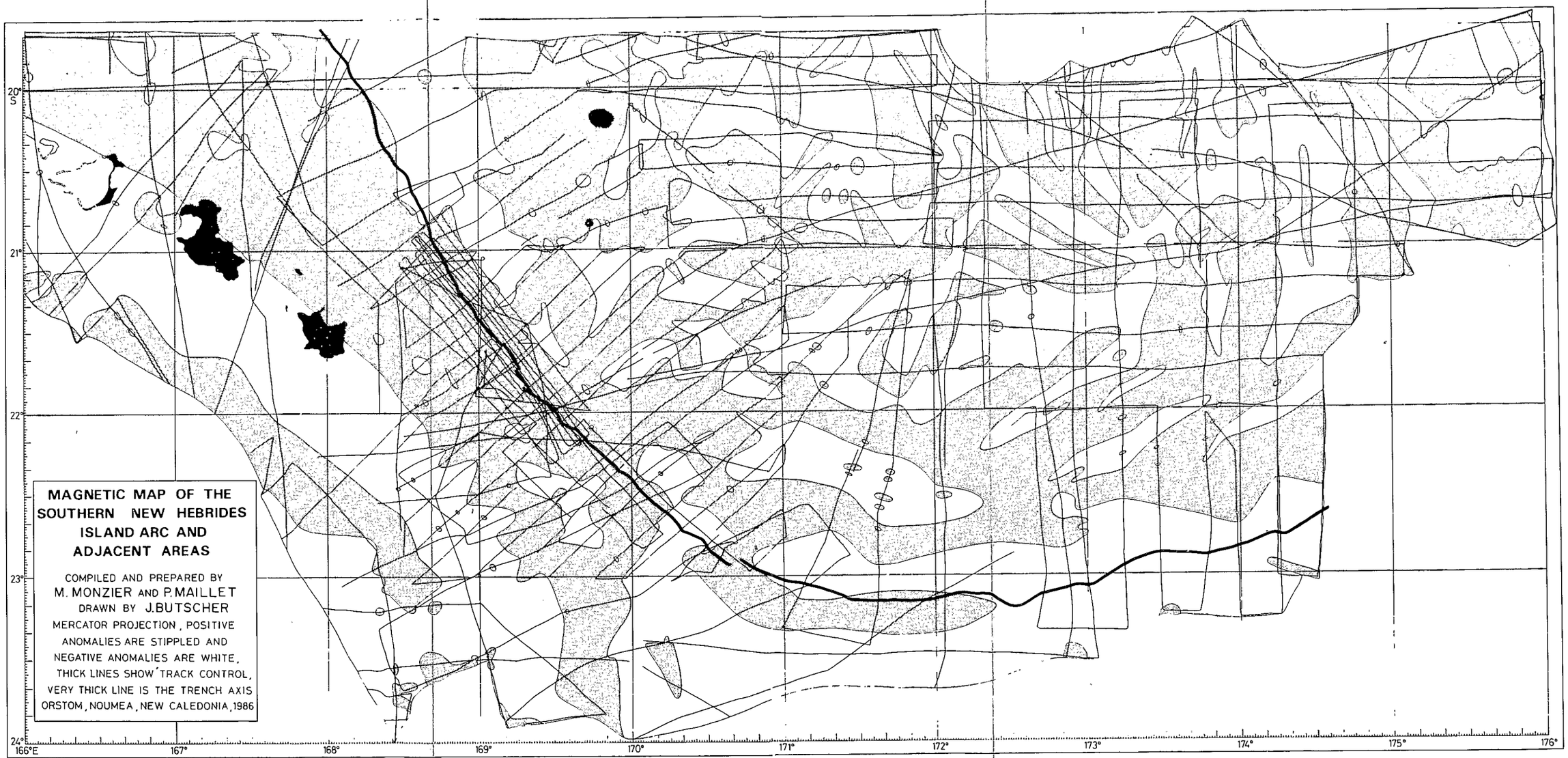

Fig. 4. Magnetic map of the southern New Hebrides island arc and southern North Fiji Basin. Positive anomalies are stippled and negative anomalies are white. Lines show track control; the heavy line marks the trench axis.

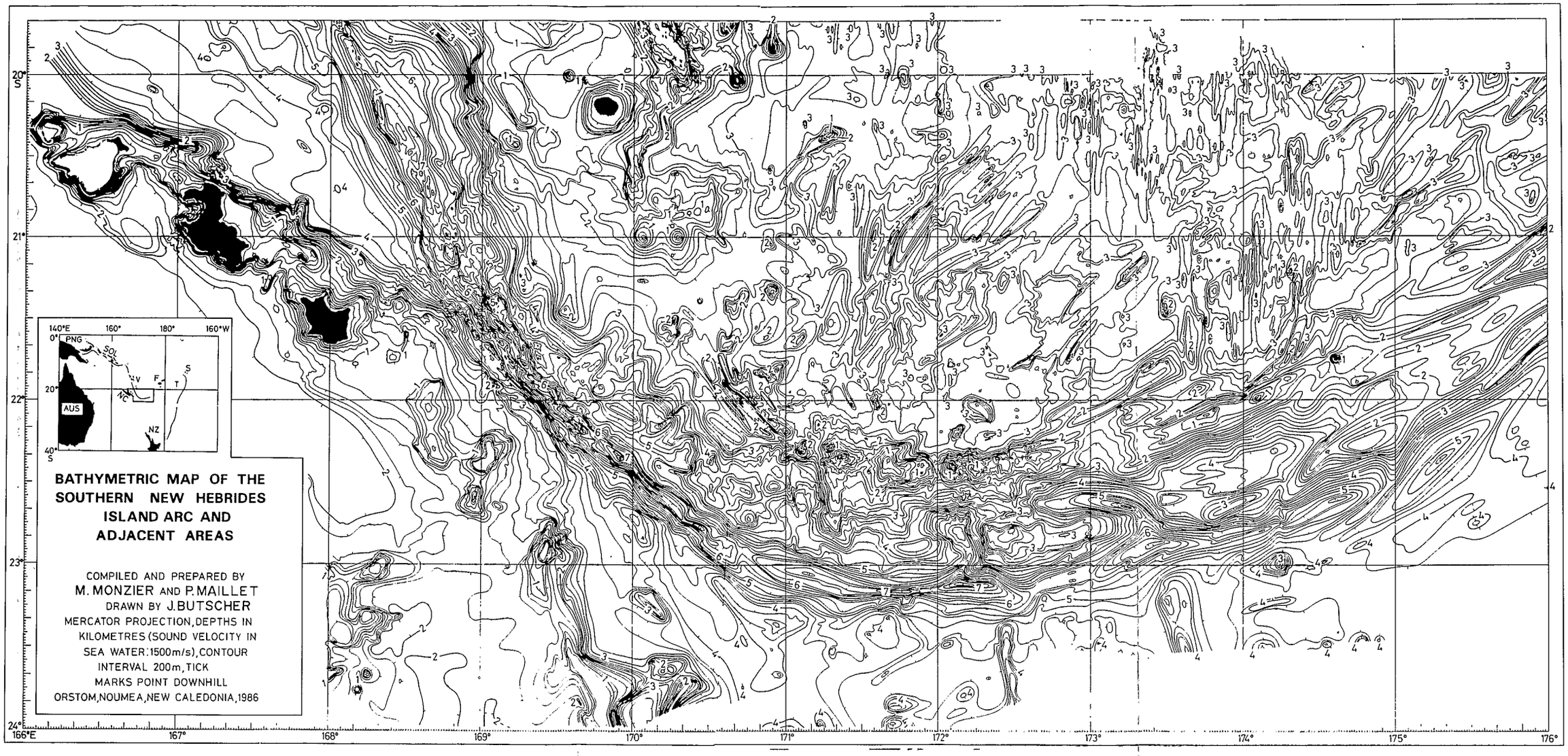

Fig. 3c. Bathymetry of the southern New Hebrides island arc and southern North Fiji Basin. Depths in kilometres; contour interval 200 m; tickmarks point downhill.

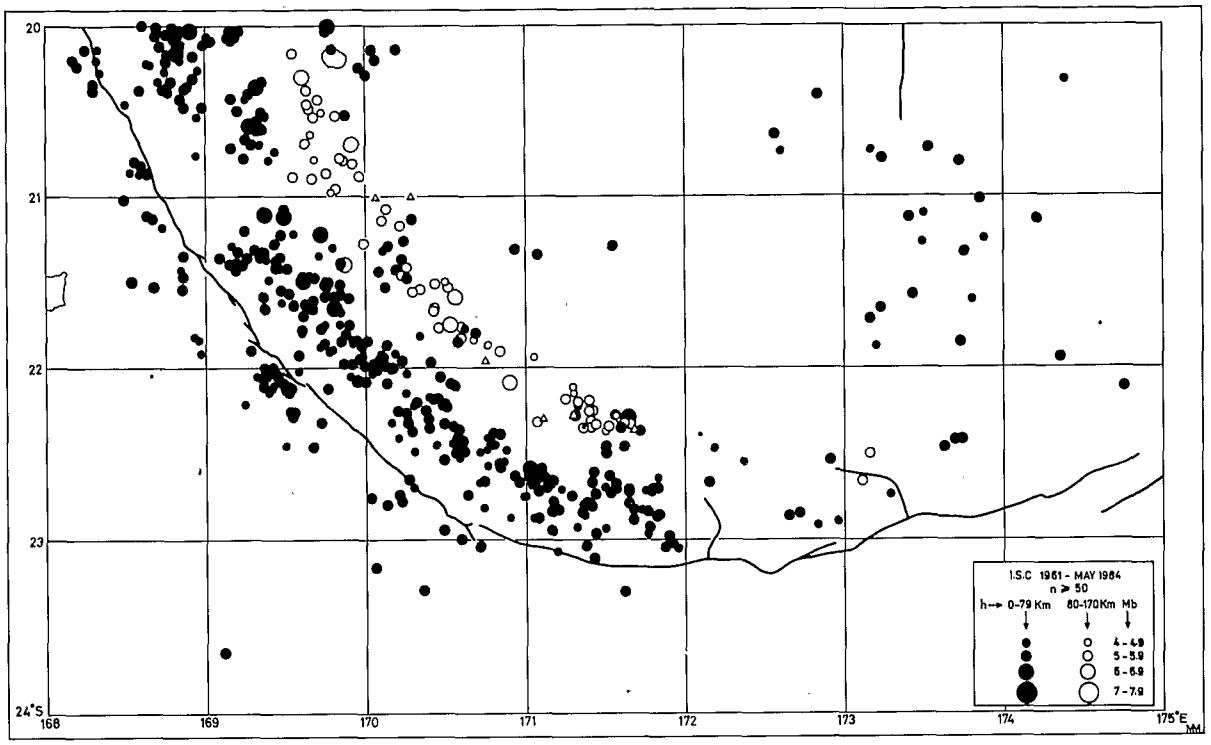

Fig. 5. Shallow and intermediate seismicity recorded in the southern New Hebrides Arc and southern North Fiji Basin (ISC, 1961–1984). Black dots—$0 < h < 79$ km; white dots—$80 < h < 170$ km (h = hypocenter depth). Size of dots proportional to M_b magnitude. Open triangles—seamounts.

structural directions on Fig. 3c. These N135°E anomalies are interpreted as magnetic remnants of the ancient NFB spreading system, active before 3 Ma.

Seismicity

Shallow seismicity

By comparison with the rest of the NHA, the width of the shallow seismicity zone abruptly shortens south of 21°S (Louat et al., 1982, 1988; Monzier et al., 1984b), and almost vanishes at 172°E, 23°S (Fig. 5). As noted before, this limit corresponds to the southeasternmost extension of the positive magnetic anomaly linked to the trench, which reaches its greatest depth in the whole southern arc there.

Shallow epicenters from the southern NHA, recorded at the DZM seismological station, Mount Dzumac, New Caledonia, exhibit a P-wave containing a wide range of dominant frequencies (1–10 Hz; Fig. 6, see inset). Plotted in Fig. 6 are the DZM-recorded epicenters which show the highest (dots) and lowest (circles) frequencies, deleting all intermediate data. Clearly, north and south of 21°45′S, most epicenters give respectively low and high frequencies at the DZM station.

Louat et al. (1988) have proposed a large-scale model linking seismicity and frequency content with the coupling between the converging plates. The area where the trench begins to bend eastwards (i.e. between 21°S and 22°S) also corresponds to the incipient collision of the Loyalty Islands Ridge with the southern New Hebrides Arc (Daniel et al., 1986; Fig. 3). There, the coupling between the two converging plates increases, and the width of the shallow seismicity zone narrows (Fig. 5). Such observations may be linked to the existence, in the uppermost part of the downgoing (and along-strike-bent) slab of a great density of normal faults, which increase the compressive stresses perpendicularly to the trench axis.

On the southern NFB, all earthquakes recorded by the ISC (International Seismological Centre)

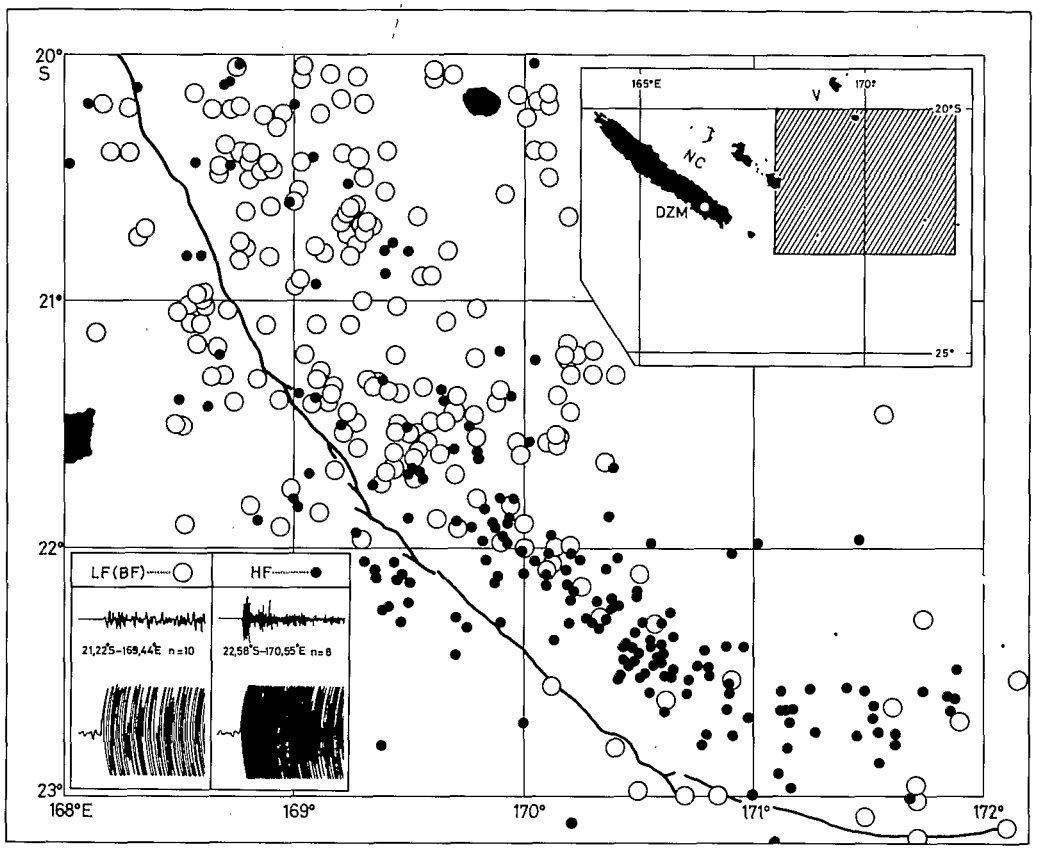

Fig. 6. Distribution of shallow seismicity (1975–1983; $h < 80$ km; $4.8 < M_b < 5.7$) in the Southern New Hebrides Arc. All events are recorded at the DZM (Mount Dzumac) seismological station (New Caledonia), and are distinguished according to their low-frequency (open circles—LF) or high-frequency (black dots—HF) P-waves.

between 1961 and 1984 are shallow-depth events (Fig. 5). Most of them are located between 173–174° E, 20°40′–22° S, i.e. in the area where the two southernmost segments of the NFB spreading ridge are offset (Figs. 3c and 4), indicating an active, though scattered, seismicity.

Intermediate-depth seismicity (80–350 km)

There is a clear limit at 20° S in the along-strike arc distribution of intermediate-depth earthquakes (Louat et al., 1982). North of 20° S, 80–170 km deep and 170–350 km deep events have been recorded between 1961 and 1984. On the contrary, south of 20° S, no deeper earthquake (170–350 km) occurred during this period. This shortening of the Benioff zone presumably corresponds to a southward extension of the subduction since 2 Ma (Louat et al., 1982; Monzier et al., 1984b; Louat et al., 1988).

According to Fig. 5, the intermediate seismicity seems to disappear near 171°40′E, 22°20′S. However, two intermediate epicenters are located near 173°10′E, 22°40′S. They should be related to the hinge fault zone tearing the downgoing slab in this area, as proposed by Monzier et al. (1984b).

Focal mechanisms

Plotted on Fig. 7 are the centroid moment tensor solutions (CMTS) of 46 earthquakes ($M_b >$ 5.1) recorded in the area since 1977 (Dziewonski and Woodhouse, 1983; Dziewonski et al., 1983a, b; Dziewonski et al., 1983–1986; Giardini, 1984; Dziewonski et al., 1987). Parameters of these earthquakes are listed in Table 1. The location of foci is given by the ISC bulletins, except for the most recent events (nos. 39–46 in Table 1) determined by the PDE/NEIC (Preliminary De-

TABLE 1

List of focal mechanism parameters for earthquakes shown in Fig. 7

										T axis		P axis		NP 1		NP 2	
N°	D	M	Y	LAT	LONG	H		n	Mb	AZ	PL	AZ	PL	STK	DP	STK	DP
1	01	08	77	-20.49	169.65	112		241	5.6	307	31	152	57	005	18	227	77
2	01	05	79	-21.22	169.72	077		541	6.2	340	27	226	38	018	41	281	83
3	08	03	80	-22.67	171.42	036		410	5.9	347	59	186	30	300	17	089	75
4	22	07	80	-20.30	169.61	131		435	6.1	266	22	092	68	352	23	178	67
5	24	10	80	-21.95	170.09	046		381	5.8	021	65	225	23	333	23	127	69
6	25	10	80	-22.09	170.13	033		371	5.7	016	69	221	19	324	27	124	65
7	25	10	80	-21.78	169.60	027		408	5.7	036	67	230	23	330	23	136	68
8	17	02	81	-21.59	169.36	013		325	5.4	073	77	238	13	323	32	151	58
9	19	02	81	-21.55	169.47	024		303	5.7	270	51	173	06	297	52	052	62
10	22	02	81	-22.11	174.76	041		318	5.9	087	37	193	19	236	49	136	79
11	24	02	81	-21.40	169.15	034		237	5.4	045	76	234	13	327	32	142	58
12	20	06	81	-20.09	169.02	058		293	5.5	084	82	245	08	332	37	158	53
13	20	06	81	-21.38	169.44	042		319	5.6	106	12	211	52	232	45	348	66
14	06	07	81	-22.29	171.64	114*		510	6.3	318	38	190	38	345	30	254	90
15	29	07	81	-21.61	169.67	041		393	5.8	057	69	228	21	312	24	140	66
16	23	08	81	-22.09	170.90	102		251	6.0	302	38	193	23	331	45	071	81
17	06	09	81	-21.50	169.61	036		393	6.0	050	45	214	44	225	08	132	90
18	17	09	81	-22.54	170.49	030		362	5.7	348	71	211	14	318	33	111	60
19	21	09	81	-22.33	170.49	040		239	5.6	024	54	204	36	295	09	114	81
20	21	09	81	-22.22	170.48	045		287	5.9	332	71	207	11	315	36	104	58
21	16	11	81	-22.11	169.52	027		377	5.7	041	01	213	89	132	44	311	46
22	24	11	81	-22.50	170.57	018		392	5.7	009	65	206	24	309	22	111	69
23	04	03	82	-22.42	173.69	053		272	5.6	313	63	174	21	291	28	071	68
24	20	05	82	-20.24	168.20	026		389	5.8	075	11	223	77	173	34	339	56
25	18	06	82	-22.70	171.83	056		241	5.6	063	82	177	03	259	42	094	49
26	17	07	82	-21.72	173.16	013		325	5.5	139	28	230	03	278	69	181	73
27	22	08	82	-20.61	169.35	068		285	5.5	190	81	069	05	167	41	332	50
28	09	09	82	-22.05	169.38	042		225	5.5	056	27	258	61	123	19	334	73
29	15	09	82	-21.43	169.19	038		204	5.1	108	75	263	14	344	32	178	59
30	05	10	82	-22.78	171.17	046		171	5.4	357	49	189	40	327	08	094	85
31	06	10	82	-22.70	171.13	049		152	5.1	337	54	197	29	329	24	091	77
32	17	04	83	-20.72	169.16	032		367	5.4	161	45	289	31	327	29	223	82
33	05	07	83	-22.59	171.02	038		411	6.0	277	11	178	40	325	54	221	71
34	07	07	83	-22.58	170.84	048		298	5.5	006	82	197	07	289	38	106	52
35	04	09	83	-20.96	169.81	103		271	5.5	277	38	090	52	033	08	184	83
36	24	02	84	-21.28	169.99	100		222	5.5	337	31	165	59	055	14	250	76
37	16	03	84	-20.53	169.87	043		151	5.2	252	03	162	09	297	82	207	85
38	03	06	84	-22.64	171.88	028		197	5.3	089	01	179	19	222	76	316	77
39	15	11	84	-22.02	170.95	105		394	6.3	PDE	338	42	207	36	356	27	093	86
40	14	01	85	-22.18	170.08	035		061	5.1	PDE	012	71	217	17	319	29	121	62
41	09	06	85	-21.56	170.40	149		093	5.3	PDE	341	21	227	47	028	39	278	75
42	07	08	85	-20.62	169.73	102		042	5.4	PDE	331	44	106	36	137	25	037	86
43	22	08	85	-22.06	169.46	033		057	5.2	PDE	254	25	092	64	329	21	170	70
44	28	08	85	-22.16	171.14	124		060	5.3	PDE	305	52	071	24	118	32	002	75
45	15	01	86	-21.28	170.10	150		030	6.2	PDE	004	46	234	32	017	28	122	83
46	10	02	86	-21.59	170.40	101		171	5.8	PDE	307	49	037	00	094	58	340	58
						*29	pP-P										

termination of Epicenters/National Earthquakes Information Center) bulletins.

Shallow seismicity (0–79 km)

On the outer trench slope (nos. 21, 28 and 43)

These events correspond to normal faults, parallel to the trench, cutting the downgoing plate crust. They occur especially near the collision zone between the Loyalty Islands Ridge and the NHA.

On the inner trench slope

Predominant thrust-faulting accounts for the plunging of the India–Australia Plate beneath the NHA, all along the trench curvature, between 169° E and 172° E.

However, between 20° S and 21° S, this type of mechanism is scarce (nos. 12–27), and corresponds to events distant from the trench. These earthquakes mark a detachment zone (Louat et al., 1988), characterized by low-stress accumulation and low-frequency P-waves (cf. supra and Fig. 6). By contrast, south of 21° S, such mechanisms are more frequent and correspond to events closer to the trench (coupled zone with high-stress accumulation and high-frequency P-arrivals; Louat et al., 1988).

The direction of relative convergence move-

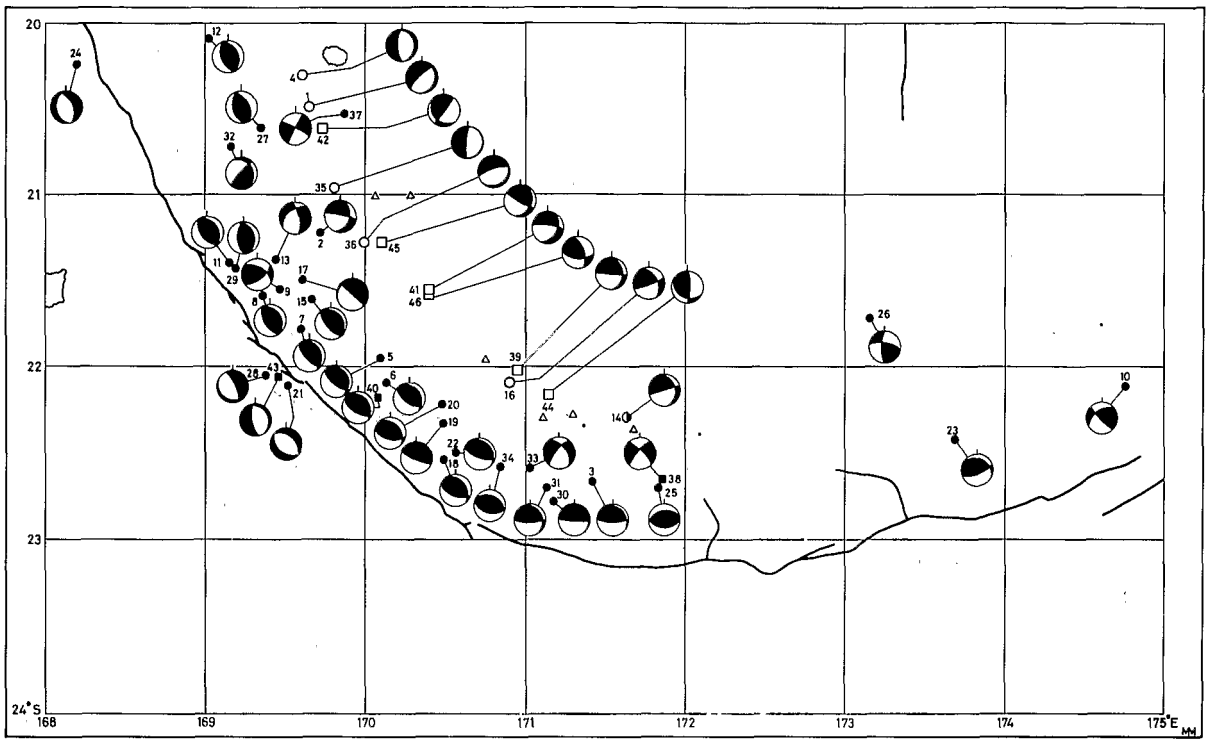

Fig. 7. Simplified focal mechanism solutions (CMTS) for earthquakes recorded in the southern New Hebrides arc and North Fiji Basin since 1977. Black dots (ISC) and black squares (PDE)—shallow (0–79 km) events; white dots (ISC) and white squares (PDE) —intermediate (80–170 km) events; open triangles—seamounts. Parameters of earthquakes are listed in Table 1.

ment given by these mechanisms always remains perpendicular to the trench, i.e. it varies from c. N65–70°E to true north from 20°S to 22°45′S. However, the convergence direction of the India–Australia/New Hebrides plates is c. N70°E (Dubois et al., 1977; Isacks et al., 1981; Coudert et al., 1981). Consequently, in the southern arcuate portion of the New Hebrides subduction zone (i.e. south of 22°S), the strike-slip component of the convergent movement has to be accommodated by left-lateral faults, which should trend N70°E and affect the arc and back-arc areas (Fitch, 1972; Beck, 1983; Maillet et al., 1986a).

Some shallow epicenters located on the upper part of the inner trench slope (nos. 2, 32, 33, 37 and 38) have solutions corresponding not to thrust movements but to steep or even subvertical normal faulting with a variable strike-slip component. Among them, two mechanisms (nos. 33 and 38) may be correlated to the numerous N165°E dextral accidents which affect the Matthew–Hunter ridge (Fig. 3c).

At the rear of the Matthew–Hunter ridge

Mechanism no. 14 (Fig. 7, Table 1) deserves a special comment. According to the ISC, it corresponds to an intermediate earthquake ($H = 114$ km). However, considering its pP–P = 29 km, it is more probably a shallow event, and actually the most powerful one recorded in the area between 1961 and 1984 ($M_b = 6.3$, $M_s \geqslant 7$). We interpret it as a subvertical N74°E accident, with a senestral strike-slip component. Another mechanism, not reported on Fig. 7, relative to a recent shallow event located at the same spot (April 16, 1987; lat. = 22.28°S, long. = 71.82°E, $H = 33$ km, $M_b = 5.6$), also gives a solution close to the one of event no. 14, i.e. a subvertical N72°E accident with a senestral strike-slip component.

To the east of 173°E

Only three mechanisms have been determined since 1977 (nos. 26, 23 and 10; Table 1). Mechanism no. 26 (strike-slip) does not clearly correlate with the bathymetric structures of Fig. 3c. Mecha-

nism no. 23 corresponds to a N–S compression movement affecting the Hunter fracture zone near 174°E. Mechanism no. 10 may result from a N56°E senestral strike-slip.

Thus, the Hunter fracture zone, near 174–175°E, is characterized by a low-level shallow seismicity, reflecting a submeridian compression component, linked to senestral strike-slip movements which parallel the easternmost extensions of the trench.

Intermediate seismicity

There is a large range of mechanisms in the intermediate seismicity, considering the solutions of Table 1. However, these mechanisms confirm that numerous and various faults shear the arcuate downgoing slab, as a consequence of its subduction into a mantle, the characteristics of which are probably influenced by the proximity of the NFB spreading system.

Mechanisms nos. 16 and 39 (Fig. 7; Table 1) support the hypothesis of a slab sheared by hinge faults roughly oriented N70°E, as proposed by Monzier et al. (1984b).

Discussion and conclusion

The synthesis of published data with the new ones discussed in this paper suggests the following geodynamic reconstruction of the New Hebrides Arc/North Fiji Basin junction during the past 3 Ma.

Ancient magnetic anomalies (i.e. 2′ and older) recorded in the central and southern NFB show a N135°E orientation, indicating that a N135°E spreading system was active before 3 Ma. Auzende et al. (1988c) propose that a N150°E spreading ridge was present in the NFB between 8 and 3 Ma. Moreover, some N135°E magnetic lineations (possibly anomalies 4A and 5) recognized in the northwestern NFB, near 171°E, 14°S (Pelletier et al., 1988) may be linked to the same spreading system, which would have thus affected the whole NFB.

While this former NFB spreading system was active, i.e. before 3 Ma, the southern arcuate termination of the New Hebrides subduction zone lay near Anatom island. Although no actual morphological feature can be associated with this former trench limit (Louat et al., 1988), the disappearance of the Coriolis back-arc troughs south of Anatom island, together with conspicuous N45°E structural lineaments controlling their southern termination near 170°20′E, 20°20′S, support the hypothesis of a former N45°E transform zone in this area.

The coeval activity of the New Hebrides subduction zone with the former N135°E NFB spreading system led to an unstable geodynamic state, because of differing convergence and divergence rates. Structural consequences of the mutual interactions of both phenomena appear in the whole area. Most of them trend N45°E (Fig. 3c). For example, it has already been noted that south of Anatom island N45°E en-échelon fault zones seem to act as a structural control of the southern termination of the Coriolis back-arc troughs. Such oblique structures also affect the inner wall of the New Hebrides trench near 170°E, 22°S. On the southern NFB, these N45°E directions underline the 3000 m isobath, around 172°E, 21°S (Fig. 3c). They are interpreted as fossil transform faults related to the former N135°E spreading ridge, like the N45°E directions recognized between 175–176°E, 20–21°S. Moreover, similar structural directions correspond to the direction of the active fracture zone separating the two limbs of the actual NFB spreading ridge between 173°E, 21°30′S and 175°E, 20°S.

Around 2 Ma, a major change occurred in the morphology of the subduction zone near 21°S, through a southward extension of the subduction (Louat et al., 1988). This propagation may explain the marked difference in the maximum depth of the Benioff zone between the region north of Anatom (300 km) and the south of this island (200 km). It may also partly account for the lack of a well defined volcanic chain between Anatom island and Matthew volcano (Fig. 3c).

In addition, the presence of c. N–S-oriented magnetic anomalies (namely 2, J and 1), in the central and southern NFB, clearly marks a new spreading stage following the NW–SE system. Its beginning can be reasonably dated at c. 2 Ma (i.e. slightly before the age of anomaly 2). It has been

shown that two limbs of this spreading system coexist south of 20°S. As indicated above, it is considered that the N174°05′E limb is regressing, whereas the N173°25′E limb is propagating to the south, as suggested by the fan shape of its bathymetric (Fig. 3c) and magnetic (Fig. 4) contours. This may indicate that the first stage of the N–S spreading system took place near the N174°E meridian, at least south of 20°S.

The proposed present-state configuration of the area studied appears on Fig. 8, which synthesizes the main data presented above.

The actual NFB spreading system, c. N–S-oriented, succeeds to a former one, oriented N135–150°E, which left the numerous N45°E structural directions recognized on Fig. 3c. These directions correspond to ancient transform faults linked to this former spreading system, which can be tracked by the presence of N135°E magnetic anomalies (Fig. 4), perpendicular to these ancient transform faults. This recent (c. 2 Ma) rearrangement of the NFB manifests one of its main characteristics, i.e. its geodynamic unstability, still effective in its southern part, as indicated by the geometry of the spreading zones between 20°S and 21°45′S. The N173°25′E limb is propagating southward, while the N174°05′E limb is dying.

A roughly N45°E-oriented fracture zone separates these two spreading segments, corresponding to an evolutionary transform zone (*ETZ* on Fig. 8). However, the presently active transform fault between these two spreading limbs trends N70°E, as a consequence of the general N70°E direction of the relative movement between the major plates in the area. Similarly oriented N70°E oblique spreading is supposed to affect the southern NFB submeridian ridges, at least south of 20°S.

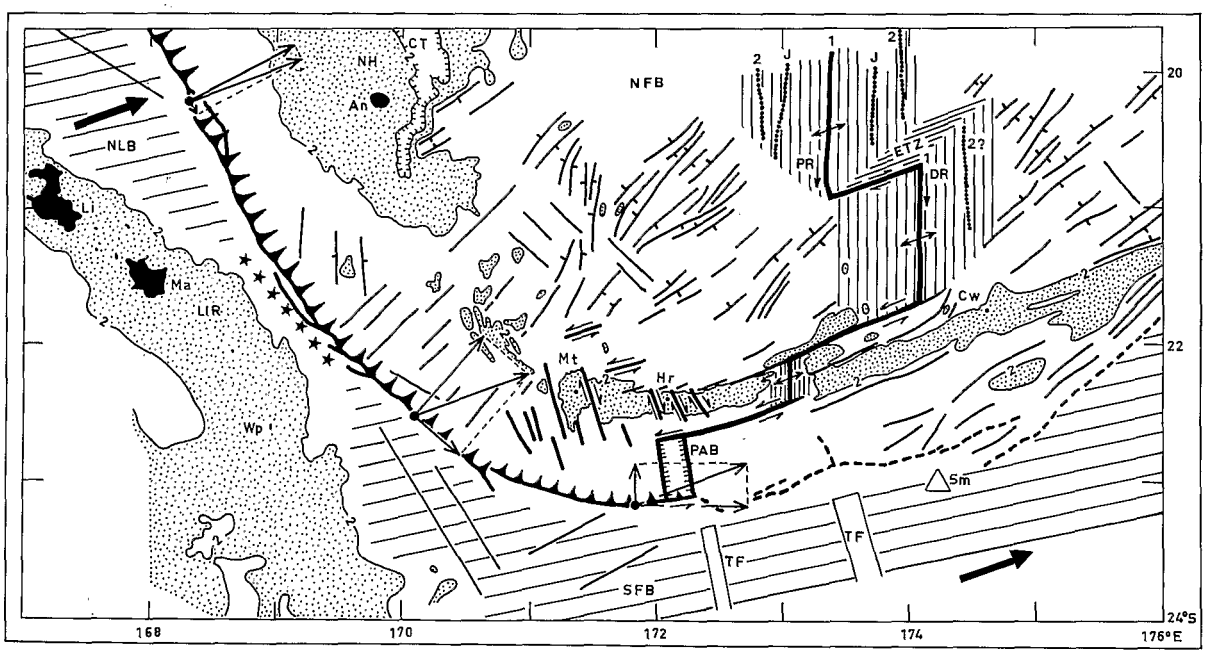

Fig. 8. Proposed geodynamic configuration of the southern junction between the New Hebrides Arc and the North Fiji Basin. Bathymetry in km. Stippled areas correspond to 0–2 km deep ridges. Toponyms: *LIR*—Loyalty Islands Ridge; *Li*—Lifou; *Ma*—Mare; *Wp*—Walpole; *NLB*—North Loyalty Basin; *NH*—New Hebrides island arc; *An*—Anatom, *CT*—Coriolis back-arc troughs; *Mt*—Matthew volcano; *Hr*—Hunter volcano; *Cw*—Conway; *NFB*—North Fiji Basin; *SFB*—South Fiji Basin; *TF*—old transform faults on the South Fiji Basin; *Sm*—seamount. Geodynamic keys: large black arrows show the general N70°E movement of the Australia–India Plate relative to the New Hebrides. The convergence vector in three different trench locations is deduced according to its two normal components. Stars point out the collision zone between *LIR* and *NH*. The active plate boundary is marked by a heavy line, on *NFB*, and by a heavy line with tick marks along the New Hebrides trench. Identified magnetic anomalies are shown along the southern *NFB* spreading zones (hatched area). *PAB*—pull-apart basin; *PR*—propagating rift; *DR*—dying rift; *ETZ*—evolutionary transform zone. See text for discussion.

The junction between spreading and convergent movements is realized between 22°S and 23°S by the functioning of two transitional structures outlined on Fig. 8.

Near 173°E, 22°10'S, the presence of a small segment in expansion is postulated. As noted before, there is a conspicuous break in the morphology of the Matthew–Hunter ridge in this area (Fig. 3c). Though apparently seismically inactive (Fig. 5), this NFB southernmost expanding area may mark the onset of a nascent northward-propagating rift. In the near future, this could coalesce with the N173°25'E southward-propagating rift, after the disappearance of the present N174°05'E dying rift.

It has already been noted that, between 171°E and 173°E, the Matthew–Hunter ridge is affected by numerous N165°E dextral strike-slip faults. These movements may have induced the formation of a pull-apart basin (Rodgers, 1980) between Hunter volcano and the easternmost termination of the trench, as proposed on Fig. 8.

However, the existence of this pull-apart basin, as well as of the small expanding area near 173°E, 22°S, remains to be ascertained by detailed bathymetric mapping and geophysical surveys.

Finally, it is probable that the incipient collision of the Loyalty Islands Ridge with the NHA will significantly change the above proposed geodynamic sketch in the future.

Acknowledgements

We are indebted to captains and crews of R/V "Vauban", R/V "Coriolis" and R/V "Jean Charcot". Thanks are also due to J. Butscher and P. Ribere for drafting.

References

Auzende, J.M., Eissen, J.P., Caprais, M.P., Gente, P., Gueneley, S., Harmegnies, F., Lagabrielle, Y., Lapouille, A., Lefèvre, C., Maillet, P., Mazé, J.P., Ondréas, H., Schaaf, A. and Singh, R., 1986a. Accrétion océanique et déformation dans la partie méridionale du bassin Nord-Fidjien: résultats préliminaires de la campagne océanographique SEAPSO III du N/O Jean-Charcot (décembre 1985). C.R. Acad. Sci. Paris, 303, II, 1: 93–98.

Auzende, J.M., Lagabrielle, Y., Schaaf, A., Gente, P. and Eissen, J.P., 1986b. Tectonique intraocéanique décrochante à l'ouest des îles Fidji (Bassin Nord-Fidjien), Campagne SEAPSO III du N/O Jean-Charcot. C.R. Acad. Sci., Paris, 303, II, 3: 241–246.

Auzende, J.M., Eissen, J.P., Lafoy, Y., Gente, P. and Charlou, J.L., 1988a. Seafloor spreading in the North Fiji Basin (Southwest Pacific). Tectonophysics, 146: 317–352.

Auzende, J.M., Honza, E. and the scientific party of the Kaiyo 87 cruise, 1988b. L'accrétion récente dans le Bassin Nord-Fidjien: premiers résultats de la campagne franco-japonaise Kaiyo 87. C.R. Acad. Sci., Paris, 306, II: 971–978.

Auzende, J.M., Lafoy, Y. and Marsset, B., 1988c. Recent geodynamic evolution of the North Fiji Basin (SW Pacific). Geology 16 (10): 925–929.

Beck, Jr., M.E., 1983. On the mechanism of tectonic transport in zones of oblique subduction. Tectonophysics, 93: 1–11.

Brocher, T.M. and Holmes, R., 1985. Tectonic and geochemical framework of the Northern Melanesian Borderland: an overview of the KK820316 Leg 2 objectives and results. In: T.M. Brocher, (Editor), Geological Investigations of the Northern Melanesian Borderland. Circum-Pac. Counc. Energy Miner. Resourc., Houston, Tex. Earth Sci. Ser., 3: 1–11.

Carney, J.N., Macfarlane, A. and Mallick, D.I.J., 1985. The Vanuatu island arc: an outline of the stratigraphy, structure and petrology. In: A.E.M. Nairn, F.G. Stehli and S. Uyeda (Editors), The Ocean Basins and Margins, Plenum Press, New York N.Y., Vol. 7A, pp. 683–718.

Charvis, P., Pelletier, B. and Ruellan, E., in prep. The northern New Hebrides back-arc troughs: history and relation with the North Fiji Basin based on tectonic and magnetic studies.

Cherkis, N.Z., 1980. Aeromagnetic investigations and sea-floor spreading history in the Lau basin and northern Fiji plateau. UN ESCAP, CCOP/SOPAC Tech. Bull., 3: 37–45.

Coudert, E., Isacks, B.L., Barazangi, M., Louat, R., Cardwell, R., Chen, A., Dubois, J., Latham, G. and Pontoise, B., 1981. Spatial distribution and mechanisms of earthquakes in the southern New Hebrides arc from a temporary land and ocean bottom seismic network and from worldwide observations. J. Geophys. Res., 86: 5905–5925.

Daniel, J., Collot, J.Y., Monzier, M., Pelletier, B., Butscher, J., Deplus, C., Dubois, J., Gérard, M., Maillet, P., Monjaret, M.C., Récy, J., Renard, V., Rigolot, P. and Temakon, S.J., 1986. Subduction et collisions le long de l'arc des Nouvelles-Hébrides (Vanuatu): résultats préliminaires de la campagne SEAPSO (Leg 1). C.R. Acad. Sci. Paris, 303, II, 9: 805–810.

Dubois, J., Launay, J., Récy, J. and Marshall, J., 1977. New-Hebrides trench: subduction rate from associated lithospheric bulge. Can. J. Earth Sci., 14: 250–255.

Dziewonski, A.M. and Woodhouse, J.H., 1983. An experiment in systematic study of global seismicity: centroid-moment tensor solutions for 201 moderate and large earthquakes of 1981. J. Geophys. Res., 88: 3247–3271.

Dziewonski, A.M., Friedman, A., Giardini, D. and Woodhouse, J.H., 1983a. Global seismicity of 1982: centroid-moment

tensor solutions for 308 earthquakes. Phys. Earth Planet. Inter., 33: 76–90.

Dziewonski, A.M., Friedman, A. and Woodhouse, J.H., 1983b. Centroid-moment tensor solutions for January–March 1983. Phys. Earth Planet. Inter., 33: 71–75.

Dziewonski, A.M., Franzen, J.E. and Woodhouse, J.H., 1983–1986. Centroid-moment tensor solutions for April–June 1983 to October–December 1985. Phys. Earth Planet. Inter., 33–43.

Dziewonski, A.M., Ekström, G., Franzen, J.E. and Woodhouse, J.H., 1987. Centroid-moment tensor solutions for January–March 1986. Phys. Earth Planet. Inter., 45 (1): 1–10.

Falvey, D.A., 1978. Analysis of paleomagnetic data from the New Hebrides. Bull. Aust. Soc. Explor. Geophys., 9 (3): 117–123.

Fitch, T.J., 1972. Plate convergence, transcurrent faults, and internal deformation adjacent to southeast Asia and the Western Pacific. J. Geophys. Res., 77: 4432–4460.

Gente, P., 1987. Etude morphostructurale comparative de dorsales océaniques à taux d'expansion variés. Thèse de Doctorat, U.B.O., Brest, no. 21, 371 pp.

Giardini, D., 1984. Systematic analysis of deep-seismicity: 200 centroid-moment tensor solutions for earthquakes between 1977 and 1980. Geophys. J.R. Astron. Soc., 77: 883–914.

Isacks, B.L., Cardwell, R., Chatelain, J.L., Barazangi, M., Marthelot, J.M., Chinn, D. and Louat, R., 1981. Seismicity and tectonics of the central New Hebrides island arc. In: D.W. Simpson and P.G. Richards (Editors), Earthquake Prediction, An International Review. M. Ewing series, Vol. 4. American Geophysical Union, Washington D.C., pp. 93–116.

Kroenke, L.W., Price, R.C., Gamo, T., Jarvis, P., Johnson, L.E., Shor, A.N., Sedwick, P., Keene, J.B., Lafoy, Y. and Tyndzik, V.E., 1987. The central North Fiji Basin: Tectonic elements unveiled. AGU, Spring Meet., 1987. Eos, Trans. Am. Geophys. Union, 68 (16): 409.

Lafoy, Y., Auzende, J.M., Gente, P. and Eissen, J.P., 1987. L'extrémité occidentale de la zone de fracture fidjienne et le point triple de 16′40S—résultats du leg III de la campagne SEAPSO du N/O Jean Charcot (décembre 1985) dans le bassin nord-fidjien (SW Pacifique). C.R. Acad. Sci., Paris, 304, II, 3: 147–152.

Louat, R., Daniel, J. and Isacks, B.L., 1982. Sismicité de l'arc des Nouvelles-Hébrides. In: Contribution à l'étude géodynamique du Sud-Ouest Pacifique. Trav. Doc. ORSTOM, 147: 111–148.

Louat, R., Hamburger, M. and Monzier, M., 1988. Shallow and intermediate-depth seismicity in the New Hebrides arc: constraints on the subduction process. In: H.G. Greene and F.L. Wong (Editors), Geology and Offshore Resources of Pacific Island Arcs, Vanuatu Region. Circum-Pac. Counc. Energy Miner. Resour., Houston, Tex., Earth Sci. Ser., 8: 329–356.

Maillet, P., Monzier, M. and Lefèvre, C., 1986a. Petrology of Matthew and Hunter volcanoes, south New Hebrides island arc (Southwest Pacific). J. Volcanol. Geotherm. Res., 30: 1–27.

Maillet, P., Eissen, J.P., Lapouille, A., Monzier, M., Baleivanualala, V., Butscher, J., Gallois, F. and Lardy, M., 1986b. La dorsale active du Bassin Nord-Fidjien entre 20.00° S et 20.53° S: signature magnétique et morphologie. C.R. Acad. Sci. Paris, 302, II (3): 135–140.

Malahoff, A., Feden, R.H. and Fleming., H.S., 1982a. Magnetic anomalies and tectonic fabric of marginal basins north of New Zealand. J. Geophys. Res., 87: 4109–4125.

Malahoff, A., Hammond, S.R., Naughton, J.N., Keeling, D.L. and Richmond, R.N., 1982b. Geophysical evidence for post-Miocene rotation of the island of Viti Levu, Fiji, and its relationship to the tectonic development of the North Fiji Basin. Earth Planet. Sci. Lett., 57: 398–414.

Monjaret, M.C., Bellon, H., Maillet, P. and Récy, J., 1987. Le volcanisme des fossés arrière-arc des Nouvelles-Hébrides (campagne SEAPSO Leg 2 du N/O Jean-Charcot dans le Pacifique Sud-Ouest): datations K–Ar et données pétrologiques préliminaires. C.R. Acad. Sci. Paris, 305, II: 605–609.

Monzier, M., Collot, J.Y. and Daniel, J., 1984a. Carte Bathymétrique des Parties Centrale et Méridionale de l'Arc Insulaire des Nouvelles-Hébrides. ORSTOM, Paris.

Monzier, M., Maillet, P., Foyo Herrera, J., Louat, R., Missègue, F. and Pontoise, B., 1984b. The termination of the southern New Hebrides subduction zone (southwestern Pacific). Tectonophysics, 101: 177–184.

Pelletier, B., Charvis, P., Daniel, J., Hello, Y., Jamet, F., Louat. R., Nanau, P. and Rigolot, P., 1988. Structure et linéations magnétiques dans le coin Nord-Ouest du bassin Nord-Fidjien: résultats préliminaires de la campagne Eva 14 (août 1987), C.R. Acad. Sci. Paris, 306, II: 1247–1254.

Récy, J., Charvis, P., Ruellan, E., Monjaret, M.C., Gérard, M., Auclair, G., Baldassari, C., Boirat, J.M., Brown, G.R., Butscher, J., Collot, J.Y., Daniel, J., Louat, R., Monzier, M. and Pontoise, B., 1986. Tectonique et volcanisme sous-marin à l'arrière de l'arc des Nouvelles-Hébrides (Vanuatu, Pacifique Sud-Ouest): résultats préliminaires de la campagne SEAPSO Leg II du N/O Jean-Charcot. C.R. Acad. Sci., Paris, 303, II, 8: 685–690.

Rodgers, D.A., 1980. Analysis of pull-apart basin development produced by en-echelon strike-slip faults. In: P.F. Ballance and H.G. Reading (Editors), Sedimentation in Oblique-slip Mobile Zones. Int. Assoc. Sedimentol., Spec. Publ., 4. Oxford, Blackwell, pp. 27–41.